

# **Axions and Experiments for Detecting Dark Matter**

Madhav Garg, Dennis Shklyar, Dario Lopez

March 29, 2025

# Contents

<b>1 Acknowledgments</b>	<b>2</b>
<b>2 Overview on Dark Matter</b>	<b>3</b>
2.1 Origins . . . . .	3
2.2 Further Evidence . . . . .	4
2.3 Cosmic Microwave Background . . . . .	4
2.4 Evidence from the CMB . . . . .	5
<b>3 Axions</b>	<b>6</b>
3.1 Parity Violation and the Strong CP Problem . . . . .	6
3.2 The Peccei-Quinn Mechanism . . . . .	7
<b>4 Dark Matter Axions</b>	<b>8</b>
4.1 Creation Mechanisms . . . . .	8
4.2 Local Properties . . . . .	9
4.3 Axion Dark Matter Experiment . . . . .	10
<b>5 Solar Axions</b>	<b>10</b>
<b>6 CERN CAST Experiment</b>	<b>12</b>
<b>7 Results from other experiments</b>	<b>13</b>
<b>8 Appendix</b>	<b>15</b>
8.1 CERN CAST DETECTORS . . . . .	15
<b>9 References</b>	<b>17</b>

# **1 Acknowledgments**

- 1. Jeff Chizma (Associate Professor, Department of Physics, UFV)**
- 2. Alexander Palmeta (Assistant Professor, Department of Physics, UFV)**
- 3. Carmen Herman (Lab Instructor, Department of Physics, UFV)**
- 4. Amar Vutha (Professor, Department of Physics, University of Toronto)**

## 2 Overview on Dark Matter

### 2.1 Origins

In 1933, Fritz Zwicky discovered that galaxies within the Coma cluster were traveling much faster than predicted. Normally, galaxies closer to the cluster's center would be expected to move slower than those at the edges. However, the observed angular velocities were consistently similar across the entire cluster.

The galaxies should have been flung out of their cluster but there was some unseen gravitational force keeping them together. Fritz Zwicky saw that accounting for all the luminous matter in the cluster was not enough to explain the discrepancy, so he proposed the idea of "Dunkle Materie", which later became known as Dark Matter.

In 1970, Vera Rubin and Kent Ford studied this effect further by examining the rotation curves in the Andromeda galaxy. According to Newtonian mechanics, the angular velocity should be lower at the edges of the galaxy compared to the center. However, their observations showed otherwise. The angular velocity of matter at the edges of the galaxy was significantly higher than expected, and it remained nearly constant as they moved further from the center, as shown in Figure 1. This result not only contradicted predictions based on visible matter but also reinforced Fritz Zwicky's earlier work on dark matter. Rubin and Ford's findings helped with the widespread acceptance of the dark matter hypothesis.

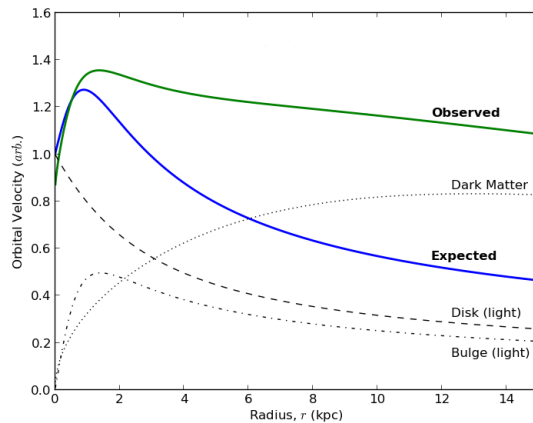


Figure 1: Discrepancy of the Angular Velocity of Matter in the Andromeda galaxy

By looking at the rotational speed of stars in a given galaxy, astronomers later found that approximately 85% of the mass of a given galaxy is made up of dark matter.

## 2.2 Further Evidence

However, many researchers remained skeptical of dark matter's existence. Some argued that the discrepancies in rotational speeds were not due to missing mass but rather indicated incomplete physical laws. They proposed modifications to Newtonian mechanics and General Relativity as alternative explanations, rather than accepting an unseen form of matter.

However, observations of the Bullet Cluster provided strong evidence in favor of dark matter. The Bullet Cluster is a system formed by the collision of two galaxy clusters, where most of the visible mass exists as interstellar gas. When the clusters merged, the gas components interacted, causing friction and heating, which led them to slow down and remain concentrated near the center. Based on this, one might expect the majority of the mass to be located in this central region.

Gravitational lensing, which relies on the bending of light by massive objects, revealed something unexpected. The regions experiencing the strongest lensing effects, and therefore containing the most mass, were not where the visible gas was concentrated. Instead, they were located at the outer edges of the system. This suggested that a significant amount of mass had passed through the collision without interacting in the same way as ordinary matter. These findings strongly support the existence of dark matter, as it behaves as a non-collisional component that does not seem to interact electromagnetically but still exerts a gravitational influence.

## 2.3 Cosmic Microwave Background

The Cosmic Microwave Background (CMB) is the afterglow of the early universe, providing a snapshot of conditions roughly 385,000 years after the Big Bang. At this stage, the universe had cooled enough for atoms to form, which allowed light to travel freely for the first time without constant scattering. This radiation carries information about the universe's early structure and composition, which has been used by researchers to study dark matter.

The CMB is typically represented as a temperature map, where red regions indicate areas that were slightly hotter than the average, while blue regions correspond to slightly cooler areas. These small temperature fluctuations ( $\approx 0.1\%$ ) reflect variations in the density of matter in the early universe, which later evolved into the large-scale structures we observe today, such as galaxies and galaxy clusters.

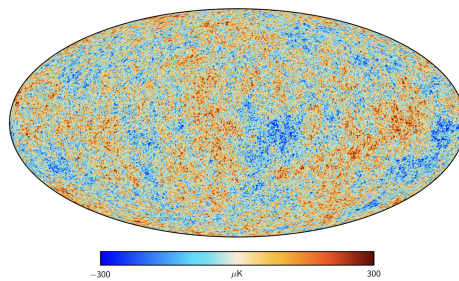


Figure 2: Cosmic Microwave Background Map

## 2.4 Evidence from the CMB

Using the map of the Cosmic Microwave Background (CMB), researchers created a graph of the temperature fluctuations relative to the multipole moment. The multipole moment  $l$  is defined as:

$$l = \frac{180^\circ}{\theta}$$

Where the angle  $\theta$  is used to measure the size of a "chunk" of a specific temperature fluctuation on the CMB map. So bigger chunks would have a larger value of  $\theta$ , which results in a smaller value of  $l$ , and vice versa.

The power spectrum  $\Delta_T^2$  of temperature fluctuations of the CMB is usually plotted as:

$$\Delta_T^2 = \frac{l(l+1)}{2\pi} C_l \langle T \rangle^2$$

$C_l \equiv$  angular power spectrum of the CMB

$\langle T \rangle \equiv$  average temperature of the CMB, which is  $\approx 2.725 K$

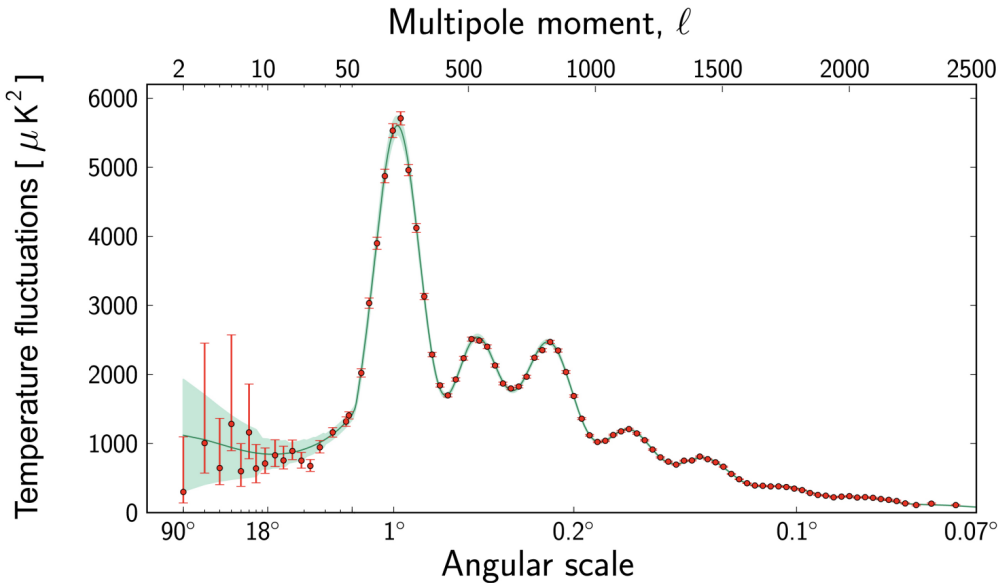


Figure 3: Power spectrum of the temperature fluctuations of the Cosmic Microwave Background measured by the Planck satellite. The red points are the measurements of  $\Delta_T^2$

It turns out (though the derivation is quite complex, and we won't dive into it here) that the odd peaks in this graph are influenced by the ratio of dark matter to ordinary matter in the universe.

In order to match the graph with the observed data, this ratio must be:

$$\frac{\Omega_{DM}}{\Omega_B} \approx 5.4$$

$\Omega_{DM}$   $\equiv$  Dark Matter Ratio

$\Omega_B$   $\equiv$  Baryonic Matter Ratio

It turns out that ordinary matter makes up only a small fraction of the observable universe. The number is approximately 5%. The ratio of dark matter is approximately 27% and the remaining value is Dark Energy, which we won't go in depth in this paper, but represents approximately 68% of all of the mass-energy content of the universe.

This report will focus on axions as a potential candidate for dark matter. However, it's important to note that there are other theoretical approaches being explored by different research groups. These include: modifications to General Relativity, supersymmetry, the little Higgs models, extra dimensions, and MACROS. These topics will not be discussed in this report.

## 3 Axions

### 3.1 Parity Violation and the Strong CP Problem

Axions are theoretical particles proposed to resolve the Strong CP problem in quantum chromodynamics (QCD). In the context of CP symmetry, C represents charge conjugation, which transforms a particle into its antiparticle, while P represents parity, which inverts the spatial coordinates of a system. If CP symmetry holds, flipping all charges and mirroring the system should result in the same physical behavior.

Initially, CP symmetry was believed to be fundamental and conserved by all forces in the Standard Model (electromagnetic, weak, and strong). However, in 1956, Tsung-Dao Lee and Chen-Ning Yang pointed out that no experimental evidence confirmed parity conservation in weak interactions. They proposed that weak interactions might violate parity, which was later confirmed in 1957 by the famous Wu experiment.

The Wu experiment, led by Chien-Shiung Wu at Columbia University, provided the first direct evidence of parity violation. Wu and her team studied the beta decay of cobalt-60 atoms, which emit electrons as they decay. By cooling the atoms to extremely low temperatures (about 3000<sup>th</sup> of a degree above absolute zero) and aligning their spins with a strong magnetic field, they observed that electrons were preferentially emitted in one direction. This asymmetry proved that the weak

interaction violates parity, which was a result that shook the physics community.

After this discovery, physicists initially believed that CP symmetry was still a true symmetry of nature. However, in 1964 the Fitch-Cronin experiment demonstrated CP violation in the weak interaction through the decay of neutral kaons. This raised a deeper problem: the Standard Model allows CP violation in weak interactions, but it also predicts that CP should be violated in strong interactions as well. Yet, experimental results suggest that CP remains conserved in strong interactions. This discrepancy is known as the Strong CP problem. For reference, we have provided the QCD Lagrangian below.

$$\mathcal{L}_{QCD} = \bar{\psi}_i (i\gamma^\mu D_\mu - m_i) \psi_i - \frac{1}{4} G_{\mu\nu}^a G^{a\mu\nu}$$

$\bar{\psi}_i$  ≡ The quark field of flavor i.(Up, down, strange, etc)  
 $m_i$  ≡ The mass of the quark of flavor i  
 $\gamma^\mu$  ≡ Gamma matrices from Dirac theory.  
 $D_\mu$  ≡ The covariant derivative that includes gluon fields  
 $G_{\mu\nu}^a$  ≡ The gluon field strength tensor

The correction to the Lagrangian would look like:

$$\mathcal{L}_{QCD} = \frac{-1}{4} G_{\mu\nu} G^{\mu\nu} + \theta \frac{g^2}{32\pi^2} G_{\mu\nu} \tilde{G}^{\mu\nu} + \bar{\psi} (i\gamma^\mu D_\mu - me^{i\theta' \gamma_5}) \psi$$

$\theta$  ≡ Unitless parameter  
 $g$  ≡ The coupling constant for the strong force

The term  $\theta \frac{g^2}{32\pi^2} G_{\mu\nu}^a \tilde{G}^{a\mu\nu}$  explicitly breaks CP symmetry. In principle,  $\theta$  can take any value from 0 to  $2\pi$ . However, experiments, particularly neutron electric dipole moment (nEDM) measurements, indicate that:

$$\theta < 10^{-10}. \quad (1)$$

Such a small value is interesting: why should nature choose  $\theta$  so close to zero? This is the Strong CP problem, which suggests the need for a deeper mechanism that naturally explains why  $\theta$  is so small.

### 3.2 The Peccei-Quinn Mechanism

In 1977, Roberto Peccei and Helen Quinn came up with the solution to this problem in the form of axions. These particles would have a very small mass, no charge, and would be a spin zero pseudo-scalar odd charge parity Boson. The term axion came from the name of a laundry detergent, as the scientists hoped it would clean up the mess.

The mass range of axions varies depending on their type. QCD axions, in particular, must have been produced in vast numbers. Despite their extremely light mass, their sheer abundance allows them to exhibit properties consistent with dark matter. Their low mass also ensures a long lifetime, making them relatively stable, which is another key characteristic of dark matter. These axions are expected to decay into photons within the X-ray spectrum.

The next section will explore how axions could account for the dark matter we observe in the universe.

## 4 Dark Matter Axions

### 4.1 Creation Mechanisms

These axions are proposed as a candidate for dark matter, and they are created in two different ways, thermally and non-thermally. We will be focusing on non-thermally produced axions as it generates the vast majority of dark matter, while thermally produced axions are constrained by cosmological observations.

The number of axions produced thermally depends on the temperature and the details of the QCD phase transition, which is the point in the early universe when the temperature dropped low enough for quarks and gluons to interact. Thermal axions are mostly produced at energies of around  $100\text{MeV}$ .

Since axions are the result of symmetry breaking, they can be produced non-thermally via the misalignment mechanism. When the universe was created, the axion's field acquired a random initial value, leading to oscillations around the minimum of its potential, which would cause an accumulation of energy density, that would result in an axion. The scalar field equation for the homogeneous axion field is  $a(t) = f_a \theta(t)$ , where the cosmological expansion rate is described by the Hubble parameter  $H(t)$ , which takes the form:

$$\ddot{\theta} + 3H(t)\dot{\theta} + m_a^2(t)\sin(\theta) = 0 \quad (2)$$

We will assume the following potential to describe axions at higher temperatures:

$$V(\theta) = f_a^2 m_a^2(t)[1 - \cos(\theta)] \quad (3)$$

$$f_a \equiv \text{decay constant} \quad (4)$$

$$m_a \equiv \text{axions mass} \quad (5)$$

While the low temperatures QCD axion potential is known to be more complicated, the relevant evolution happens when the low temperature does not apply. The initial conditions are taken to be  $\theta(0) = \theta_i$  and  $\dot{\theta} = 0$ , where  $\theta_i$  is the initial misalignment angle.

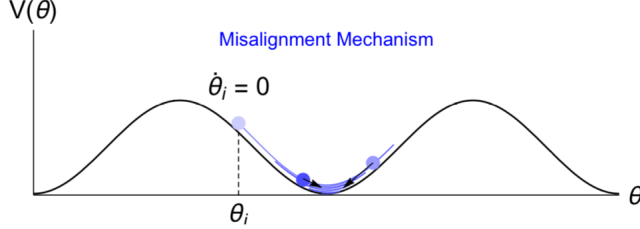


Figure 4: Schematic of the misalignment mechanism

As the Hubble parameter  $H(t)$  reached  $H \approx m_a$ , the field became dynamical and started to oscillate, its energy density is transferred into the form of non-relativistic axion particles.

These various production mechanisms; thermal and non-thermal, contribute to the overall abundance of axions in the universe, shaping their distribution as dark matter.

## 4.2 Local Properties

Assuming that these particles are real, we expect some of the properties to be the following. The local density of dark matter within our galaxy is measured to be around  $\rho = 0.4 \text{ GeV cm}^{-3}$ , so the distribution of axions should follow this. The dark matter particles should also have velocities  $\approx 300 \frac{\text{km}}{\text{s}}$ , similar to the stars that they would expect.

Assuming the expected mass range for dark matter axions is correct, it would require them to be very numerous in order to explain the effects we have seen with dark matter. These non-thermally produced axions must be non-relativistic, meaning they move slowly compared to the speed of light, in order to be proper dark matter candidates, as they need to behave according to dark matter properties. While thermally produced axions are produced with high kinetic energy, they act as relativistic particles, similar to neutrinos in the early universe.

Axion dark matter is also expected to have a persistent, but spread out density within galaxies. The local axion density is influenced by its distribution within larger cosmic structures like dark matter halos. These halos are regions of high axion density where gravitational collapse has occurred, forming structures such as filaments that also seed the formation of stars and galaxies. The spectral shape of axions is known to be a key factor for detection, as it describes how axions are distributed across different frequencies and energies. The distribution is not necessarily uniform, so researchers have to consider peaks or fine structures in the axion signal to improve the chances of identifying axions.

### 4.3 Axion Dark Matter Experiment

The Axion Dark Matter Experiment (ADMX) is a collaboration between multiple institutions, including the University of Washington, FERMILAB, LLNL, LANL, and others.

ADMX focuses on detecting dark matter axions within the mass range of  $1 \mu\text{eV}$  to  $40 \mu\text{eV}$ , which are expected to decay into photons. Although dark matter axions rarely interact with ordinary matter, they could interact in the presence of a strong electromagnetic field.

Despite no direct detection of dark matter axions, ADMX has placed constraints on their possible mass. The experiment has ruled out axions existing within the range of  $m_a \approx 2.66 \mu\text{eV}$  to  $3.33 \mu\text{eV}$ . In the future, ADMX will focus on exploring axions with masses greater than  $m_a > 3.33 \mu\text{eV}$ .

## 5 Solar Axions

Solar Axions are axions that are produced by the sun, or in the vicinity of the sun. These light axions are primarily produced from photons through the Primakoff process, and they can also convert back into photons via the same mechanism.

The Primakoff process occurs when a pseudoscalar particle, such as an axion, interacts with an external electromagnetic field, typically from a nucleus. This interaction can either generate a photon or convert a photon into an axion. This process serves as a key theoretical foundation for detecting axions, as they could transform into detectable photons when passing through strong magnetic fields. An example of the process is shown below:

$$\gamma + Z/e \rightarrow a + Z/e$$

Where:

$$Z/e = \text{Charged nucleus or electron}$$

The corresponding Feynman Diagram would be:

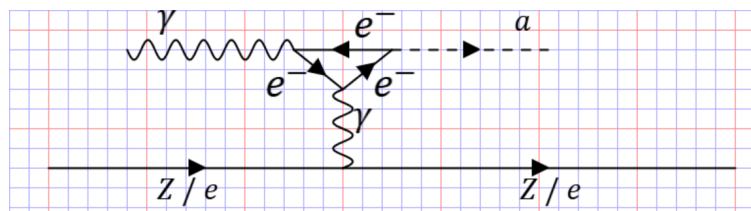


Figure 5: Primakoff process Feynman Diagram

In the Feynman diagram above, we have a photon ( $\gamma$ ) and a charged particle ( $Z/e$ ) interacting. The charged particle exchanges a virtual photon and virtual electrons in the interaction. The final state

consists of the produced axion and the original charged particle ( $Z/e$ ). This process shows the conversion of a photon into an axion through the exchange of virtual particles, in accordance with the Primakoff process.

More massive axions are produced by the Photon Coalescence process, where 2 photons are required to produce 1 axion:

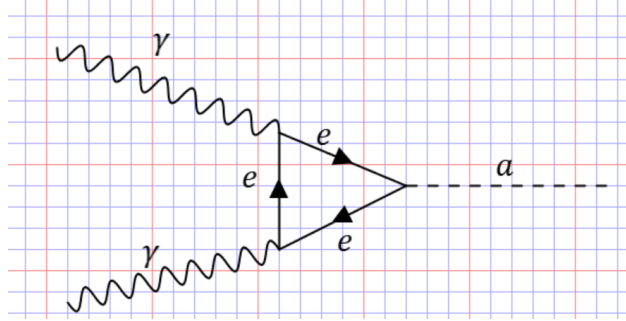


Figure 6: Photon Coalescence Feynman Diagram

Initially, 2 photons come in and via virtual electrons produce a single axion.

Another significant process for axion production is the Bremsstrahlung process. In this process, an electron interacts with a charged particle, such as a nucleus or another electron. The interaction results in the emission of an axion. This process is particularly important in stellar environments, where electrons frequently interact with charged particles in high-density conditions. In stars, these interactions lead to a continuous production of axions.

$$e + I/e \rightarrow e + I/e + a$$

We can represent this process in a Feynman diagram, where the electron exchanges a virtual particle (often a photon) with the charged particle, which leads to the production of an axion and the final state of the electron and the charged particle.

A third axion production process involves the interaction between a photon and an electron, which is the Compton process. In this interaction, the photon exchanges energy with the electron, and under certain conditions, an axion is produced. The Feynman diagram for this process typically shows the photon ( $\gamma$ ) interacting with the electron ( $e$ ), where the photon is absorbed and then re-emitted in the form of an axion. This process is important in environments like stars, where photons and electrons frequently interact. The Feynman diagram for the Compton process is shown below.

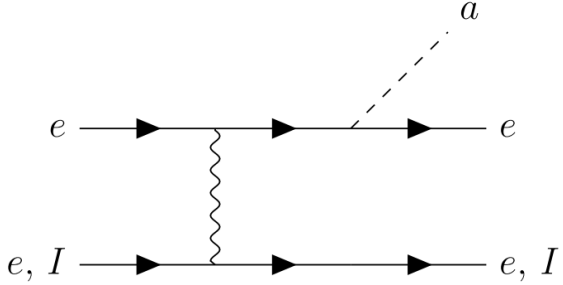


Figure 7: Bremsstrahlung process

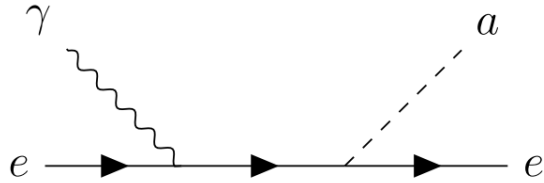


Figure 8: Compton Process

## 6 CERN CAST Experiment

Experiments such as the CERN Axion Solar Telescope (CAST) are dedicated to detecting axions. CAST is designed to search for solar axions originating from the Sun. This telescope serves as a prototype of a dipole magnet.



Figure 9: CAST Experimental Setup

The CAST telescope was designed to search for axions originating from the Sun. Since axions are theorized to decay into photons, CAST aims to detect them indirectly. CAST (Figure 9) is a magnet capable of generating a 9.5 T magnetic field. It observes the Sun for 1.5 hours at sunrise and another 1.5 hours at sunset. The superconducting magnet is maintained at a temperature of 1.8 K. The setup includes two bores, each with a diameter of 43 mm and a length of 9.26 m, with X-ray detectors attached at both ends.

The detectors used in CAST include Conventional Time Projection Chambers (TPC) (Figure 2), MICROMEsh GAseous Structure detectors (MICROMEGAS), an X-ray telescope equipped with a Charge-Coupled Device (CCD), the GridPix detector, the Relic Axion Dark Matter Exploratory Setup (RADES), and CAST-CAPP. Further details on these detectors can be found in the appendix.

Although CAST has not yet directly detected axions, it has placed significant constraints on their properties. In particular, it has set an upper limit on the axion-photon coupling parameter,  $g_{a\gamma} < 0.57 \times 10^{-10} \text{ GeV}^{-1}$ . This result indicates that axions interact extremely weakly with electromagnetism, which explains the difficulty in detecting them. CAST continues to focus on the search for ultralight axions with masses below  $m_a < 0.02 \text{ eV}$ .

## 7 Results from other experiments

Various research groups are actively working on axion detection, and their efforts are summarized in the table below. Different groups estimate axion masses spanning from eV to several keV, indicating that solar axions are exceptionally light. Their low mass implies they would be fast-moving and relativistic.

Bound	Analysis
$g_{a\gamma} \leq 7 \times 10^{-10} \text{ GeV}^{-1}$	Tokyo Axion Helioscope
$g_{a\gamma} \leq 7 \times 10^{-10} \text{ GeV}^{-1}$	SNO experimental data
$g_{a\gamma} \leq 5.7 \times 10^{-11} \text{ GeV}^{-1}$	CAST analysis (2024)
$g_{a\gamma} \leq 6.9 \times 10^{-12} \text{ GeV}^{-1}$	NuSTAR analysis (2024)

Table 1: Bounds on axion-photon and axion-electron couplings from various analyses.

Although different groups have reported varying results, they consistently indicate that the axion-photon coupling must be extremely weak. Using the results from the CAST experiment, the probability of axion-to-photon conversion can be expressed as:

$$P_{a \rightarrow \gamma} = 2 \times 10^{-21} \left( \frac{g_{a\gamma}}{10^{-12} \text{ GeV}^{-1}} \right)^2 \left( \frac{L}{10 \text{ m}} \right) \left( \frac{B}{9.0 \text{ T}} \right)^2 \quad (6)$$

From Eq. (1), it is evident that the theoretical probability of axions converting to photons is extremely small, which explains why they have not yet been detected.

Different experiments are targeting distinct mass ranges:

- **NuSTAR** focuses on detecting axions with a mass around  $m_a \approx 2 \times 10^{-7} \text{ eV}$ .
- **Tokyo Axion Helioscope** targets axions within the mass range of  $m_a \approx 0.84 \text{ eV} - 1 \text{ eV}$ .

- **Sudbury Neutrino Observatory (SNO)** estimates axion masses to be around  $m_a \approx 10\text{keV}$ .

While these experiments place the mass of axions within different ranges, they consistently suggest that the axion mass is extremely small. For comparison, the mass of an electron is  $m_e = 0.5\text{ MeV}$ , highlighting the incredibly light nature of axions.

Currently, the CERN CAST experiment is considered the most accurate in terms of constraining axion-photon couplings, and the mass of the axions.

## 8 Appendix

### 8.1 CERN CAST DETECTORS

Figure 10 shows the Time Projection Chamber (TPC), which is a gas-filled drift chamber detector designed to detect low-intensity X-ray signals. This detector consists of a large gaseous chamber and a magnetic field concentrated around the central region.

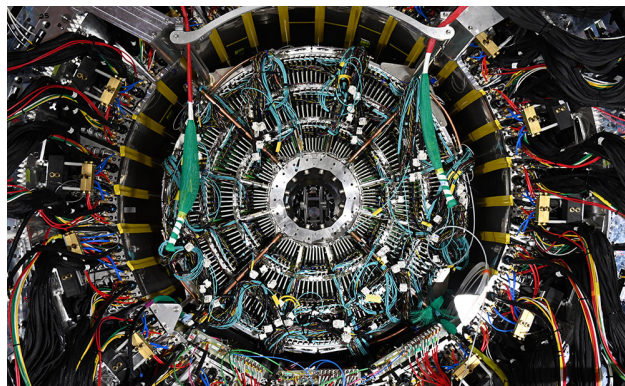


Figure 10: Time Projection detector(TPC)

Figure 11 shows the MICROMEgas detector, which is a gaseous device primarily used for measuring X-rays in the 1–10keV range. It's constructed from low-radioactivity materials, so MICROMEgas is designed to detect axions that convert into X-ray photons upon entering the detector.

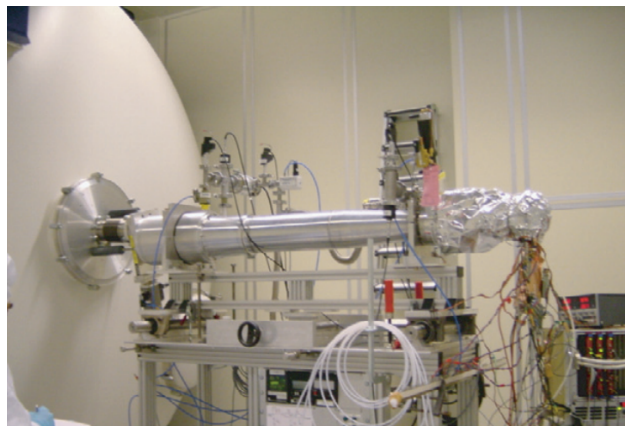


Figure 11: MicroMEsh Gaseous Structure detectors(MICROMEgas)

The Charge-Coupled Device (CCD) incorporates a pn-CCD chip positioned at the focal plane of an X-ray telescope. The pn-CCD chip functions as a sensor for detecting both light and particles. The telescope itself features a mirror system composed of 27 gold-coated nickel shells arranged in a confocal parabolic-hyperbolic structure. The largest shell measures 163 mm in diameter and the smallest is 76 mm, with the entire system having a focal length of 1.6 m. The GridPix detector enhances CAST's sensitivity to X-ray energies around 1 keV.

RADES is an experiment that began searching for axions in 2018 and has yet to yield significant results. Figure 12 displays the RADES detector before and after its coating process. This detector consists of a 316LN stainless steel cavity coated with a 30  $\mu\text{m}$  thick copper layer and is further divided into five sub-cavities.

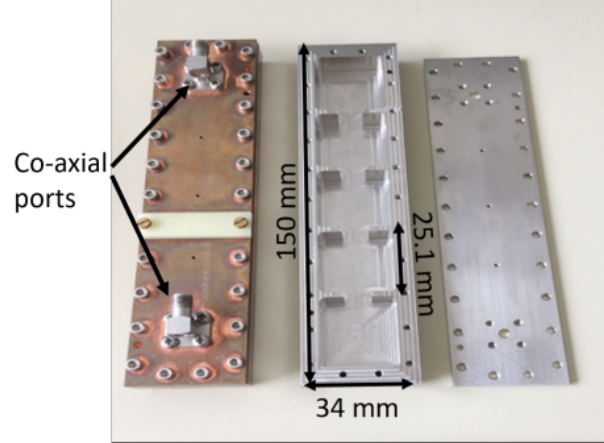


Figure 12: Relic Axion Dark Matter Exploratory Setup (RADES)

Figure 13 illustrates the CAST-CAPP detector, which consists of two parallel sapphire plates and is designed to search for axions within the 21–23  $\mu\text{eV}$  energy range.

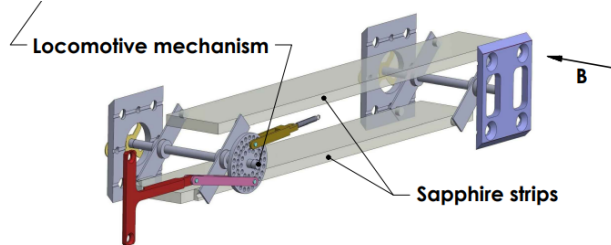


Figure 13: CAST-CAPP

## 9 References

1. O'Hare, C. A. J. et al. (2022). *Dark Matter Axion Search with Microwave Cavities*. arXiv preprint. Retrieved from <https://arxiv.org/pdf/2203.14923>
2. Gramolin, A. V., Ayala, A. L., Obrecht, J. M., & Sushkov, A. O. (2022). *Search for Axion-Like Particles with Precision Magnetometry*. Science Advances, 8(4). Retrieved from <https://www.science.org/doi/10.1126/sciadv.abj3618>
3. Fermilab News. (2019). *ADMX Experiment Places World's Best Constraint on Dark Matter Axions*. Retrieved from <https://news.fnal.gov/2019/11/admx-experiment-places-worlds-best->
4. DOE Office of Science. *DOE Explains... Dark Matter*. Retrieved from <https://www.energy.gov/science/doe-explainsdark-matter>
5. NASA. *Roman Space Telescope: Dark Matter*. Retrieved from <https://science.nasa.gov/mission/roman-space-telescope/dark-matter/>
6. ResearchGate. *Feynman Diagrams of Axion Production Processes in the Sun*. Retrieved from [https://www.researchgate.net/figure/Feynman-diagrams-of-the-different-processes-fig1\\_357703480](https://www.researchgate.net/figure/Feynman-diagrams-of-the-different-processes-fig1_357703480)
7. Nature Communications. *Article on Axion Production*. Retrieved from <https://www.nature.com/articles/s41467-022-33913-6>
8. CERN. *CAST Experiment*. Retrieved from <https://home.cern/science/experiments/cast>
9. Pettini, M. (n.d.). *Introduction to Cosmology - Lecture 10*. Retrieved from <https://people.ast.cam.ac.uk/~pettini/Intro%20Cosmology/Lecture10.pdf>
10. NASA. *WMAP - Wilkinson Microwave Anisotropy Probe*. Retrieved from <https://map.gsfc.nasa.gov/>
11. Nelson, A. E. & Scholtz, J. (2019). *New Developments in Axion Physics*. arXiv preprint. Retrieved from <https://arxiv.org/pdf/1910.08638>
12. Raffelt, G. (2008). *Astrophysical Axion Bounds*. arXiv preprint. Retrieved from <https://arxiv.org/abs/0809.0596>
13. Murayama, H. (n.d.). *Physics Beyond the Standard Model*. Retrieved from <https://tinyurl.com/5xrfrun3>